Number 3 Volume 16 September 2010 Journal of Engineering

PREDICTION OF NATURAL CONVECTION HEAT TRANSFER IN COMPLEX PARTITIONS CAVITY

Dr. SATTAR J. HABBEB
Lecturer
Mechanical Engineering Dept.
Technology University

ISRAA Y. DAOUD
Asst. Lecturer
Mechanical Engineering Dept.
Technology University

ABSTRACT

A numerical investigation has been carried out to examine the effects of insulated baffle mounted in complex cavity representing as an industrial building on flow pattern and heat transfer characteristics. The cavity is formed by adiabatic horizontal bottom, inclined upper walls and vertical isothermal walls. This problem is solved by using flow-energy equations in terms of stream-vorticity formulation in curvilinear coordinates. Two cases are considered; in the first (case 1) the insulated baffle position attached to the horizontal bottom wall of the cavity while in the second case (case 2) the insulated baffle position attached the upper inclined wall. A parametric study is carried out using following parameters: Rayleigh number from 10^3 to 10^6, Prandtl number for 0.7 and 10, baffle height (HB=0, $0.3H^*$, $0.4H^*$, and $0.5H^*$), baffle location for (LB=0.25L and 0.75L) with or without baffle in the cavity (total of 100 tests). For case 1 results show that, the flow strength generally increasing with increasing Ra values, increasing baffle height, and decreasing values of Pr, while in case 2 the same behavior of above could be show except the flow strength decreasing with increasing baffle height, also, increase Ra leads to increase the rate of heat transfer. The configuration of the cavity in case 2 leads to increase in heat transfer rate comparing with that in case 1.

KEY WORDS: natural convection, cavity with baffle

الخلاصة

تم التوسع بدراسة عددية لاختبار تأثير الحاجز المعزول الموضوع في تجويف معقد يمثل بناية صناعية على حركة الجريان وسمات انتقال الحرارة بالحمل الحر. التجويف متمثل بأسطح معزولة السطح الأفقي السفلي , السطح المائل العلوي وأسطح ثبوت درجة الحرارة العمودية. المسألة حلت باستخدام معادلات الجريان والطاقة بصيغة دالة الانسياب-الدوامية بالإحداثيات المطابقة للجسم. تم اخذ حالتين في هذه الدراسة الحالة الأولى الحاجز المعزول منطبق على السطح السفلي للتجويف بينما في الحالة الثانية يكون منطبق على السطح المائل العلوي للتجويف, المعاملات المدروسة هي:رقم رايلي من 10^3الى 10^6,رقم برانتل 0.7 و 10,ارتفاع الحاجز (HB= 0, $0.3H^*$, $0.4H^*$, $0.5H^*$) موقع الحاجز (LB=0.25L, 0.75L), لحالات مختلفة بدون وبوجود الحاجز داخل

التجويف (حوالي 100 اختبار). النتائج للحالة الأولى أوضحت أن قوة الجريان بصورة عامة تزداد مع زيادة رقم رايلي, زيادة ارتفاع الحاجز المعزول, ونقصان قيم رقم برانتل بينما في الحالة الثانية يبقى نفس التصرف أعلاه مع نقصان قوة الجريان بازدياد ارتفاع الحاجز المعزول. كذلك زيادة قيم رقم رايلي تؤدي إلى زيادة معدل انتقال الحرارة. تركيب التجويف في الحالة الثانية يؤدي إلى زيادة معدل انتقال الحرارة مقارنة بالحالة الأولى.

INTRODUCTION

Heat transfer and fluid flow inside complex cavity with or without baffles has not been investigated widely due to geometric complexity. This case study represented as an industrial building, numerous references deal with enclosures with flat straight walls due to its huge application in engineering like as, solar-collectors and cooling system of electronic devices. Especially for the cooling low powered laptop computers, monitors and TV. These are always complex interaction between the finite fluid content inside the enclosure with enclosure walls. This complexity increase when the wall becomes inclined, wavy or content baffles distributed in the enclosure. In the past, a great number of studies have focused on a vertical of cavity configuration formed with straight walls, mostly cavities of square, rectangular, trapezoidal and parallelogram cross sections. Representative reference that have divulged these efforts are condensed in Iyican et al (1980), Van Doormaal et al (1981), Law et al (1991), and Peric (1993). In these works buoyancy-induced flows are considered in the physical system and descriptive mathematical methodologies in the analysis or the experimental procedures in the laboratory are outlined.

The method of transformed coordinates was originally proposed in Jang et al (2003) as a tool to solve heat transfer problems in the presence of irregular surface of all kinds. This method is not limited to heat transfer problems, but is also applicable to other problems in engineering and science. Karyakin (1989) investigated transient natural convection in a trapezoidal cavity with parallel top and bottom walls and inclined side walls. Lee (1991) presented numerical results up to a Rayleigh number of 10^5 for natural convection in trapezoidal enclosure of horizontal bottom and top walls that are insulated and isothermal inclined side walls. Moukalled et al (2003) studied numerically the natural convection in a partitioned trapezoidal cavity heated from the side. In particular the effect of Rayleigh number, Prandtl number, baffle height, and buffle location on heat transfer is investigated for two boundary conditions representing buoyancy-assisting and buoyancy-opposing modes along the upper inclined surface of the cavity. Shi et al (2003) performed a numerical study in a square cavity due to thin fin on the hot wall. They concluded that heat transfer capacity on the anchoring wall was always degraded; however, heat transfer capacity on the cold wall without the fin can be promoted for high Rayleigh numbers and with fins placed in the vicinity of the insulated walls.

Tasnim et al (2005) analyzed the laminar natural convection heat transfer in a square cavity with an adiabatic arc shaped baffle. As boundary conditions of the cavity, two vertical opposite walls are kept at constant but different temperatures and the remaining two walls are kept thermally insulated. Results are presented for a range of Rayleigh number, arc lengths of the baffle, and shape parameters of the baffle. Ambarita et al (2006), studied numerically a differentially heated square cavity, which is formed by horizontal adiabatic walls and vertical isothermal walls. Two perfectly insulated baffles were attached to its horizontal walls at symmetric position. The results show that Nusselt number is an increasing function of Rayleigh number, a decreasing one of baffle length and strongly depends on baffle position. Dagtekin et al (2006), studied natural convection

heat transfer and fluid flow of two heated partitions within an enclosure have been analyzed numerically. The right side wall and the bottom wall of the enclosure were insulated perfectly while the left side wall and top wall were maintained at the same uniform temperature. The partitioned were placed on the bottom of the enclosure and their temperatures were kept higher than the non-isolated walls. The effects of position and heights of the partitions on heat transfer and flow field for Rayleigh number range from 10^4 to 10^6 have been investigated.

Bilgen (2002) investigated numerically the laminar and turbulent natural convection in enclosures with partial partitions. Vertical boundaries are isothermal and horizontal boundaries were adiabatic. Various geometrical parameters were: aspect ratio, partition position, height of the partition and Rayleigh number, the results is reduced in terms of the normalized Nusselt number as a function of the Rayleigh number and other non dimensional geometrical parameters. An experimental study of low level turbulence natural convection in an air filled vertical partitioned square cavity was conducted by Ampofo (2004). The dimension of the cavity, which was 0.75*0.75*1.5, resulted in two dimensional flow. The hot and cold walls of the cavity were isothermal at 50 and 10 $^{\circ}C$ respectively giving a Rayleigh number of $1.58*10^9$. The local velocity and temperature were systematically measured at different locations in the cavity and both mean and fluctuation quantities are presented.

The objective of this study is to examine numerically the natural heat transfer in complex geometry such as industrial building with or without baffles distributed in the cavity. Moreover to study the effect of Rayleigh number, Prandtl number and configuration of these baffles such as height and position for two cases, baffle attached the horizontal bottom wall of the cavity or attached the upper inclined wall on the characteristics of natural convection heat transfer in the cavity.

PHYSICAL MODEL

The conjugate problem under present consideration is depicted in **Fig. 1,** which show a complex cavity represented in industrial buildings with insulated bottom and inclined top walls. The left wall fixed at hot temperature T_h while the right wall maintained at the cold temperature T_c, the inclination of the top surface of the cavity is fixed at 15 degree. The geometry of the cavity in this study fixed at the width of the cavity 4 times the height of the left vertical wall. Results show two cases according to the position of the baffle, which is attached to horizontal bottom wall or attached to inclined top wall of the cavity as shown in **Fig. 1.** Three baffle height (HB = $0.3H^*$, $0.4H^*$, $0.5H^*$) and two position of the baffle (LB= 0.25L, 0.75L) are studied. In all computational the baffle thickness (WB=L/30) to simulate a thin baffle. The viscose incompressible flow inside a closed cavity and a temperature distribution is described by the Navier-Stokes and energy equations for two dimension and steady. The Boussinesq approximation is used with the assumption of constant properties and negligible viscous dissipation. The governing equation in stream function- vortities formulation in dimensionless form is defined as follows:

$$\frac{\partial^2 \psi}{\partial^2 x} + \frac{\partial^2 \psi}{\partial^2 y} = -\omega \qquad (1)$$

$$\frac{\partial \omega}{\partial t}+u\frac{\partial \omega}{\partial x}+v\frac{\partial \omega}{\partial y}=\Pr\left(\frac{\partial^2 \omega}{\partial^2 x}+\frac{\partial^2 \omega}{\partial^2 y}\right)+\Pr\cdot Ra\,\theta \tag{2}$$

$$\frac{\partial \theta}{\partial t}+u\frac{\partial \theta}{\partial x}+v\frac{\partial \theta}{\partial y}=\left(\frac{\partial^2 \theta}{\partial^2 x}+\frac{\partial^2 \theta}{\partial^2 y}\right) \tag{3}$$

Hence, introducing the following non-dimensional variables:

$(x,y)=(x^{\bullet},y^{\bullet})/l \quad , \quad (u,v)=(u^{\bullet},v^{\bullet})\cdot l/a \quad , \quad \theta=(T-T_c)/(T_h-T_c)$

$\Pr=\nu/a \quad , \quad Ra=g\,\bar{\beta}\,l^3(T_h-T_c)/(a\nu)$

The study is completed with the following boundary condition:

$\theta=0$, $u=v=0.$ $\Rightarrow$*on the cold wall*

$\theta=1$, $u=v=0.$ $\Rightarrow$*on the hot wall*

$\theta_x=0$, $\theta_y=0$, $u=v=0.$ $\Rightarrow$*on the rest*

NUMERICAL PROCEDURES

The grid generation calculation is based on the curvilinear co-ordinate system applied to fluid flow as described by Thompson (1999). The transformation is as follows: $\xi=\xi(x,y)$, $\eta=\eta(x,y)$. The problem is now defined in terms of new variables:

$$\left[\lambda\cdot\psi_{\xi}+\sigma\cdot\psi_{\eta}+\alpha\cdot\psi_{\xi\xi}-2\beta\cdot\psi_{\xi\eta}+\gamma\cdot\psi_{\eta\eta}\right]/J^2=-\omega \tag{4}$$

$$\begin{aligned}\omega_t+\left[\psi_{\eta}\cdot\omega_{\xi}-\psi_{\xi}\cdot\omega_{\eta}\right]/J=\Pr\left[\lambda\cdot\psi_{\xi}+\sigma\cdot\psi_{\eta}+\alpha\cdot\psi_{\xi\xi}-2\beta\cdot\psi_{\xi\eta}+\gamma\cdot\psi_{\eta\eta}\right]/J^2\\ +Ra\cdot\Pr\cdot\left[y_{\eta}\cdot\theta_{\xi}-y_{\xi}\cdot\theta_{\eta}\right]/J\end{aligned} \tag{5}$$

$$\theta_t+\left[\psi_{\eta}\cdot\theta_{\xi}-\psi_{\xi}\cdot\theta_{\eta}\right]/J=\left[\lambda\cdot\theta_{\xi}+\sigma\cdot\theta_{\eta}+\alpha\cdot\theta_{\xi\xi}-2\beta\cdot\theta_{\xi\eta}+\gamma\cdot\theta_{\eta\eta}\right]/J^2 \tag{6}$$

Where

$$\begin{aligned}&\alpha=x_{\eta}^2+y_{\eta}^2 \quad , \quad \gamma=x_{\xi}^2+y_{\xi}^2 \quad , \quad \beta=x_{\xi}x_{\eta}+y_{\xi}y_{\eta}\\ &\lambda=\left[x_{\eta}(\alpha\cdot x_{\xi\xi}-2\beta\cdot x_{\xi\eta}+\gamma\cdot x_{\eta\eta})-y_{\eta}(\alpha\cdot y_{\xi\xi}-2\beta\cdot y_{\xi\eta}+\gamma\cdot y_{\eta\eta})\right]/J\\ &\sigma=\left[y_{\xi}(\alpha\cdot y_{\xi\xi}-2\beta\cdot y_{\xi\eta}+\gamma\cdot y_{\eta\eta})-x_{\xi}(\alpha\cdot x_{\xi\xi}-2\beta\cdot x_{\xi\eta}+\gamma\cdot x_{\eta\eta})\right]/J\end{aligned} \tag{7}$$

The boundary condition represented in the following table:

Table 1 Boundary condition in the typical case study

	ψ	θ	ω
Left wall	0	1	$-\alpha\cdot\psi_{\xi\xi}/J^2$
Right wall	0	0	$-\alpha\cdot\psi_{\xi\xi}/J^2$
Inclined wall	0	θ_{η} =0	$-\gamma\cdot\psi_{\eta\eta}/J^2$
Bottom wall	0	θ_{η} =0	$-\gamma\cdot\psi_{\eta\eta}/J^2$
Baffles	0	θ_{η} =0 , θ_{ξ} =0	$-\alpha\cdot\psi_{\xi\xi}/J^2$, $-\gamma\cdot\psi_{\eta\eta}/J^2$

The heat transfer rate by convection in a hot left wall of the cavity is obtained from the Nusselt number calculation. The local Nusselt number and average Nusselt number are expressed as:

$$Nu_l = \alpha \cdot \theta_\xi \Big/ J\sqrt{\alpha} \quad , \quad Nu_{ava} = \int_0^1 Nu_l \cdot dy \tag{8}$$

VALIDATION OF THE CODE

In order to make sure that the developed codes are free of error coding, a validation test was conducted, calculations for an air filled square cavity without baffle for Ra=10^4, 10^5, 10^6 were carried out and the results are shown in table 1. the results of the previous publication for the same problem are also presented in table. Data from the table shows that the results of the code, even through there are some differences, do agree very well with the previous works results. Those differences are not essential, the maximum difference is 1.01% and probably caused by the different grid sizes and round-offs in the computational process.

Table 2. Comparison of the present result and the previous works result.

Reference	Average Nusselt number Nu_{ave}		
	Ra =10^4	Ra =10^5	Ra =10^6
Collins (2005)	2.244	4.5236	8.8554
Shi (2003)	2.247	4.532	8.893
Bilgen (2005)	2.245	4.521	8.800
Present study	2.248	4.514	8.804

RESULTS AND DISCUSSION

In order to understand the flow pattern, temperature distribution and heat transfer characteristics of the typical case study a total of 100 cases were considered. To study the effects of the baffle position (LB = 0.25L, 0.75L), baffle height (HB = 0.3H*, 0.4H*, 0.5H*), Rayleigh number (Ra = 10^3, 10^4, 10^5, 10^6), and Prandtl number (Pr = 0.7, 10) for two cases according to the baffle, attached to the horizontal bottom wall or attached to the inclined upper wall of the cavity. Flow and temperature fields and Nusselt number are examined. Typical grid generation for the cavity represented as shown in **Fig 2**.

Flow and Temperature Fields

The flow consists of a recirculating eddy rotating clockwise, indicating that the fluid filling the cavity is moving up along both the left heated vertical wall and the top insulation inclined wall (the slope is positive) until reach to the middle of the cavity, then the flow down along the top insulation inclined wall (the slope is negative), cold right vertical wall, and horizontally to the left along the insulated bottom wall of the cavity. All results of streamline and isothermal contours are takes for Pr=0.7.

Fig. 3 shows streamline and isothermal maps in the cavity without baffles as depicted, the flow structure consists of a single eddy rotating clockwise. At low Rayleigh number values, the eye of the recirculating vortex is located at the middle of the cavity

close to the hot vertical wall of the cavity, where the largest velocities was located as shown in **Fig. 3A,** and **3C**. As Ra increase **Fig. 3E,** and **3G**, the eye of the vortex moves away from the hot wall towards the middle of the cavity and upward towards the top inclined upper wall of the cavity. In addition, at the highest Ra value $Ra=10^6$, the flow separates near the lower right corner of the cavity. For low Ra ($Ra=10^3$) **Fig. 3B**, isotherms values decrease uniformly from hot to cold wall showing dominant weak convection heat transfer. As Ra increase, the distribution of isothermal implies higher stratification levels within the cavity compare **Fig. 3B,** and **3H**, and consequently higher convection contribution.

For case 1 where the baffles attached horizontal bottom wall of the cavity, the flow pattern and isothermal contours are discussed below. **Fig. 4** and **Fig. 5** show that for LB=0.25L, HB=0.4H* and LB=0.75L, HB=0.4H* respectively. Streamlines in **Fig. 4** indicated that at the lowest Ra presented ($Ra=10^3$), the recirculating flow exhibits single vortex (**Fig. 4A,** and **4C**) located near the middle of the cavity. This vortex rotates in the clockwise direction. As Ra increase, the two vortices will be appearing in the cavity around the baffle. The left vortex close to the left hot wall (**Fig. 4E,** and **4G**) is more uniform comparing with right vortex. Increase Ra leads to distrom the right vortex which move towards the left and upper inclined wall in the cavity. Moreover, with increasing values of Ra, the flow between the baffle and the cold right wall becomes weaker as compared to the region between the baffle and the hot left wall. The colder fluid tends to stagnate in the lower right-hand section of the cavity between the baffle and right vertical wall (cold wall). Resulting in a thermally stratified region and inhibiting the penetration of the warmer fluid from the cavity left-hand section. Isotherms presented in **Fig. 4** (left side), reflect the above described flow patterns. At low Ra, variation in temperature is almost uniform over the domain. As Ra increase, convection is promoted, and isothermal contours become more distorted.

The effects of positioning of the baffle close to the cold right wall on the streamline and isotherms are depicted in **Fig. 5** for LB=0.75L, HB=0.4H*. At low Ra value **Fig. 5A,** and **5C**, the flow structure is qualitatively similar to that presented in **Fig**. **4A,** and **4C**, with small vortex behind the baffles close to the right cold wall. As Ra values increase **Fig**. **5G,** and **5E**, a more pronounced thermally stratified zone developed in the baffle cold wall region as a compared to the configuration in which the baffle is close to the hot wall (**Fig**. **4G,** and **4E**). This thermally stratified region prevents the bulk of the fluid descending a long the cold wall from penetrating the region. Moreover, to that the two vortices appear in the cavity, first is uniform as a circle close to the cold right wall and the second is similar to the ellipse shape move up to the left wall. The above described behavior is further exemplified by the isothermal plots presented in **Fig**. **5** (left side). At low Ra stratification effects are small and distribution of isotherms is more or less uniform. While as Ra increase, isotherms becomes more distorted and stratification effects are promoted. The effects of baffles height on the hydrodynamics and thermal fields are presented in **Fig**. **6** for baffle position LB=0.25L and $Ra=10^6$. Streamlines and isotherms are displayed for four different baffles height of (HB=0, 0.3H*, 0.4H*, 0.5H*). As HB increase, a weaker flow is observed in both the right and left portions of the doman, two non-similar clockwise rotating eddies are noticed in **Fig. 6C, 6E**, and **6G** with their strength lower than the single vortex flow in the cavity without baffle. For highest HB the left vortex is more uniform and dissipated between the baffle and the hot

left wall, while the right vortex is move to up and distributed to the weak flow near to the cold right wall. Isotherms presented in **Fig. 6** (left side) are in accordance with above finding and clearly show the decreases in the convection heat transfer through the spread of the isotherms.

For case 2 where the baffles attached upper inclined wall of the cavity, the flow pattern and isothermal contours are discussed below. **Fig**. **7** and **Fig**. **8** show that for LB=0.25L, HB=0.4H* and LB=0.75L, HB=0.4H* respectively. Streamlines in **Fig**. **7** indicated that at the lowest Ra (Ra=10^3), the recirculating flow exhibits two clockwise rotating vortices with some communication between them (**Fig**. **7A**). As Ra increase, the deformation of the vortices increase, moreover, the increasing Ra values, the eye of the vortex in the right hand portion of the domain moves upward and to the left as a result of increasing stratification level in the lower right portion of the cavity. Isotherms presented in **Fig**. **7** (left side) reflect the above described flow pattern. At low Ra, variations in temperature are almost uniform over the domain, If Ra increase, convection is promoted and stratification effects are increased. The effects of positioning the baffle closer to the cold vertical wall on the streamlines and temperature fields are depicted in **Fig**. **8** for LB=0.75L, HB=0.4H*. At low Ra values the flow structure is qualitatively similar to the previous **Fig**. **7** but in this case the weak flow region could be show between the baffle and the cold right wall. As Ra values increase **Fig**. **8E,** and **8G**, stratification levels increase and isotherms become more distorted in the baffle cold wall region as compared to the configuration in which the baffle is closer to the hot left wall (**Fig**. **7E,** and **7G**). This indicates stronger convection caused by higher buoyancy effects as a result of the longer distance the flow travels before encountering the baffle. Isothermal contours in this case are similar to that in **Fig**. **7** with some difference in shape and behavior of flow in the cavity due to increase the position of the baffle from the hot wall. The effects of baffles height on the hydrodynamics and thermal fields are presented in **Fig**. **9** for baffle position LB=0.25L and Ra=10^6. Streamlines and isotherms are similar to that in case 1 (**Fig. 6**) but it show weaker flow in both sides of the baffle, more decrease in convection heat transfer, and more deformation in streamline and isotherms.

Heat transfer parameter

Local Nusselt number distribution along hot wall is presented in **Fig. 10** for case 1 the Nu_l levels increase with increasing Ra indications higher convection contribution. If the position of baffle is increase the Nu_l increase because the temperature difference along the hot wall is increase for constant Ra expect for Ra=10^6 because the buoyancy effect become more declare and huge. This behavior also shows in case two **Fig. 11** with small difference in shape of the curve and its values. For low Ra, the Nu_l is low too because the limited of convection heat transfer in this case. **Fig. 12** shows the Nu_l distribution along the hot wall for different height baffle and for two cases. Increase HB values leads to decrease the Nu_l because the temperature difference is decrease too. In case 2 (**Fig. 12** right side) increase height baffle leads to increase the values of Nu_l comparing with its values in case 1 (**Fig. 12** left side) due to the location of the baffle in the cavity. **Fig 13** represents the average Nusselt number distribution according to the Rayleigh number for two cases. Figures show that for log scale axis where the relation is

linear and if the height of the baffle increase the slope of the curve is increase too, this description is applied for two cases.

Maximum stream function (flow strength)

The maximum absolute values of the stream function displayed in table **3** for case 1 (baffle attached the horizontal bottom wall) and to different value of Pr=0.7 and 10. Indicated that the flow strength (maximum velocity in the domain) generally increase with increasing baffle height and decreasing values of Pr, moreover, the strength of flow increase with Ra due to an increase in temperature difference. **Table 4** show that for case 2 (baffle attached the upper inclined wall), indicated that the flow strength generally decreases with increasing baffle height and increasing values of Pr due to the increase in the fluid viscosity. Moreover the strength of the flow increases with Ra values increase due to an increase in temperature difference and consequently in buoyancy forces.

Table 3. Maximum absolute values of stream function for baffles attached the horizontal bottom wall.

Ra	Without baffles	Baffles Height HB					
		0.3 H^*	0.4 H^*	0.5 H^*	0.3 H^*	0.4 H^*	0.5 H^*
		LB =0.25 L			LB =0.75 L		
Pr = 0.7							
10^3	0.2520	0.2277	0.26714	0.3310	0.2535	0.2675	0.3289
10^4	1.8887	1.79598	1.9339	2.1504	1.9554	1.9808	2.0804
10^5	11.1519	7.2596	7.3242	7.4226	6.7567	6.7617	6.773
10^6	15.7261	16.3829	17.6351	19.0268	16.883	16.944	17.123
Pr = 10							
10^3	0.0176	0.0156	0.0180	0.0219	0.0178	0.0188	0.02366
10^4	0.1394	0.12527	0.1327	0.1437	0.1392	0.1419	0.1519
10^5	1.1110	1.2202	1.2854	1.3788	1.3602	1.3793	1.4368
10^6	7.6564	7.0533	7.2353	7.7474	7.1792	7.1182	7.4256

Table 4. Maximum absolute values of stream function for baffles attached the inclined upper wall.

Ra	Without baffles	Baffles Height HB					
		0.3 H^*	0.4 H^*	0.5 H^*	0.3 H^*	0.4 H^*	0.5 H^*
		LB =0.25 L			LB =0.75 L		
Pr = 0.7							
10^3	0.2520	0.1949	0.1935	0.1852	0.2466	0.2451	0.2435
10^4	1.8887	1.5714	1.5131	1.4467	1.9469	1.9409	1.9342
10^5	11.1519	6.9733	5.9200	4.8871	6.8875	6.8742	6.8690
10^6	15.7261	16.1176	14.3799	13.0812	14.9814	13..9628	13.1340
Pr = 10							
10^3	0.0176	0.0139	0.0136	0.0135	0.0171	0.0170	0.0168
10^4	0.1394	0.1159	0.1143	0.1107	0.1365	0.1356	0.1347
10^5	1.1110	1.1179	1.0917	1.0513	1.3398	1.3329	1.3252
10^6	7.6564	6.4921	5.6038	5.0103	7.2502	7.3050	7.3016

CONCLUSION

For case 1 results show that, the flow strength generally increasing with increasing Ra values, and decreasing values of Pr, while in case 2 the same behavior of above could be show except the flow strength decreasing with increasing baffle height. Also, increase Ra leads to increase the rate of heat transfer, the configuration of the cavity in case 2 leads to increase in heat transfer rate comparing with that in case 1 as shown in figures and tables.

REFERENCES

- Amberite H., Kishinami K., Daimaruya M., Saitoh T., Takahashih H., and Suzuki J., "Laminar natural convection heat transfer in an air filled square cavity with two insulated baffles attached to its horizontal walls", Jouornal of Thermal science and engineering, vol. 14,no. 3, 2006.
- Ampofo F., "Turbulent natural convection in an air filled partitioned square cavity", Int. J. of Heat and Fluid Flow, 25(2004)103-114.
- Bilgen E., "Natural convection in enclosures with partial partitions", Journal of Renewable Energy, 26(2002)257-270.
- Bilgen E., "Natural convection in cavities with a thin fin on the hot wall", Int. J. Heat and Mass Transfer, 48(2005)3493-3505.
- Dagtekin I., and Oztop H., "Natural convection heat transfer by heated partitions within enclosure", Int. J. of heat and mass transfer, vol. 28, no. 6, 2006, pp.823-834.
- Iyican L., Bayazitoglu Y., and Witte L.C. , " An analytical study of natural convection heat transfer within a trapezoidal enclosure", ASME . J. Heat transfer, 102(1980), 640-647.
- Iyican L., Bayazitoglu Y., and Witte L.C. , " An experimental study of natural convection in trapezoidal enclosure", ASME . J. Heat transfer, 102(1980), 648-653.
- Karyakin Y.E., "Transient natural convection in prismatic enclosures of arbitrary cross section", Int. J. of heat and mass transfer, Vol. 32, no. 6(1989)1095-1103.
- Jang J.H., Yan W.M., and Liu H.C., "Numerical convection heat and mass transfer a long a vertical wavy surface", Int. J. of heat and mass transfer, 46(2003)1075-1083.
- Law S.W., Gani R., and Symons J.G., "Experimental and numerical studies of natural convection in trapezoidal cavities", ASME . J. Heat transfer, 111(1991), 372-377.
- Lee T.S., "Numerical experiments with fluid convection in tilted nonrectangular enclosure", Journal of Numerical heat transfer, A, vol. 10, (1991)487-499.
- Moukalled F., and Darwish M., "Natural convection in a partitioned trapezoidal cavity heated from the side", Journal of Numerical heat transfer, Part A-43(2003)543-563.
- Peric M.," Natural convection in trapezoidal cavities", Journal of Numerical heat transfer, Part B-24(1993)213-219.

- Shi, and Khodadi, "Laminar natural convection heat transfer in a differentially heated squre cavity due to a thin fin on the hot wall", J. heat transfer 125(2003)624.
- Tasnim S.H., and Collins M., "Suppressing a natural convection in a differentially heated square cavity with an arc shaped baffle", Int. J. of heat and mass transfer, 32(2005)94-106.
- Thompson J. F., Bharat K. S., and Weatherill N. P., " Handbook of grid generation", 1999 by CRC Press LLC.
- Van Doormaal J.P., Raithby G.D., and Strong A.B., "Predication of natural convection in non-rectangular enclosure using orthogonal curvilinear coordinates", Journal of Numerical heat transfer, 4(1981)21-38.

NOMENCLATURE:

SYMBOLS	TITLES	UNITS
a	Thermal diffusivity	m/sec^2
g	Gravitational acceleration	m/sec^2
H	Cavity height (left vertical wall)	m
HB	Baffle height	m
H^*	Height of the cavity at the location of the baffle	m
J	Jacobian	-----
L	Cavity width	m
LB	baffle position	m
Nu	Nusslet number	-----
Pr	Prandtl number (ν/a)	-----
Ra	Rayleigh number ($g.\beta'.(T_h - T_c).L^3/\nu.a$)	-----
T	Temperature	$^{\circ}C$
t	Time	sec
u,v	Dimensionless velocity	-----
WB	Baffle thickness	-----
x, y	Dimensionless coordinates	-----
GREEK SYMBOLS		
θ	Dimensinless temperature	-----
β'	Thermal expansion coefficient	1/K
$\alpha,\beta,\gamma,\lambda,\sigma$	Transformation functions	-----
ξ , η	Dimensionless curvilinear coordinates	-----
ψ	Stream function	-----
ω	Vorticity	-----
ν	Kinematics viscosity	m^2/sec
SUBSCRIPTS		

ave	Average
c	Cold wall
h	Hot wall
l	Local
max	Maximum value
x , y, ξ , η	Derivative relative to x, y, ξ , and η respectively.

SUPERSCRIPT

•	Dimensional form

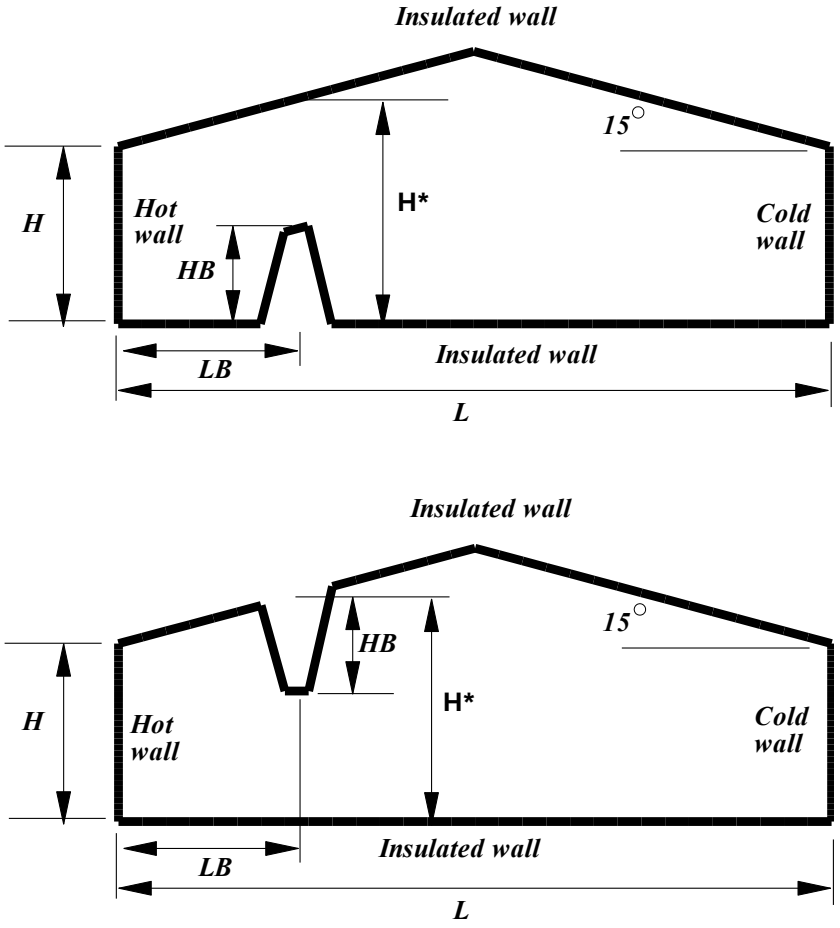

Fig. 1 Typical cavity with boundary conditions for two cases
A. Case 1 (baffle attached to the horizontal bottom wall)
B. Case 2 (baffle attached to the upper inclined wall)

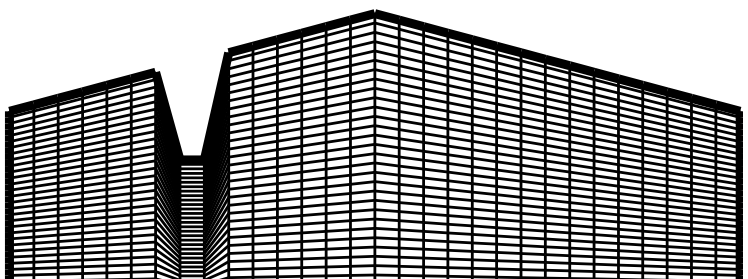

A Ra =10^3 B

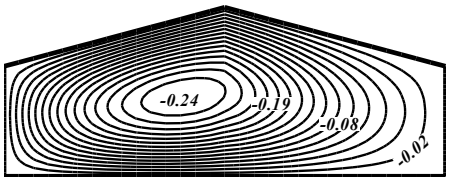

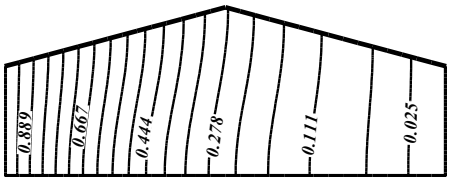

C Ra =10^4 D

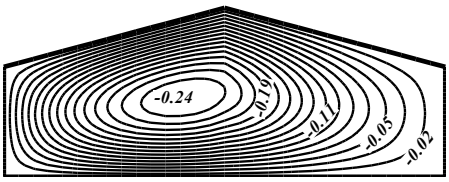

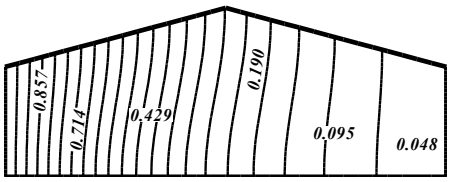

E Ra =10^5 F

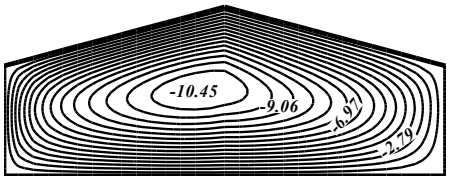

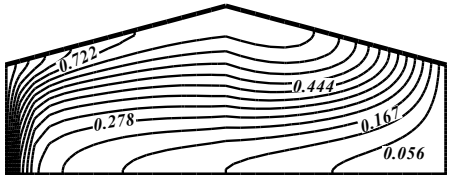

G Ra =10^6 H

A **Ra =10^3** **B**

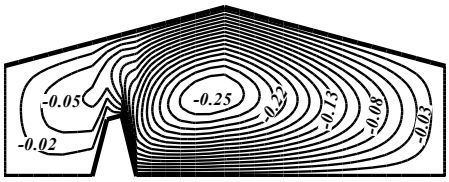

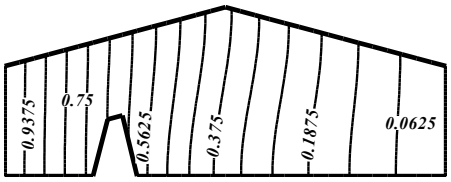

C **Ra =10^4** **D**

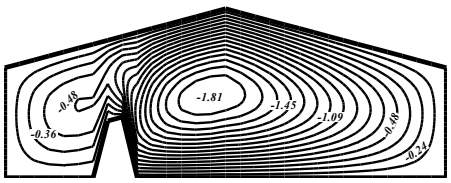

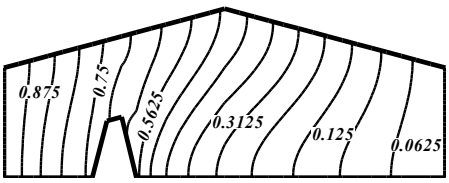

E **Ra =10^5** **F**

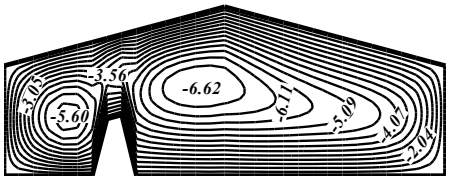

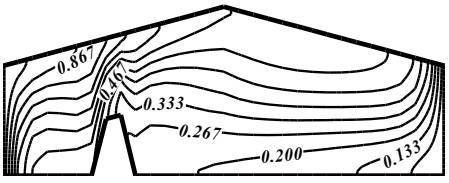

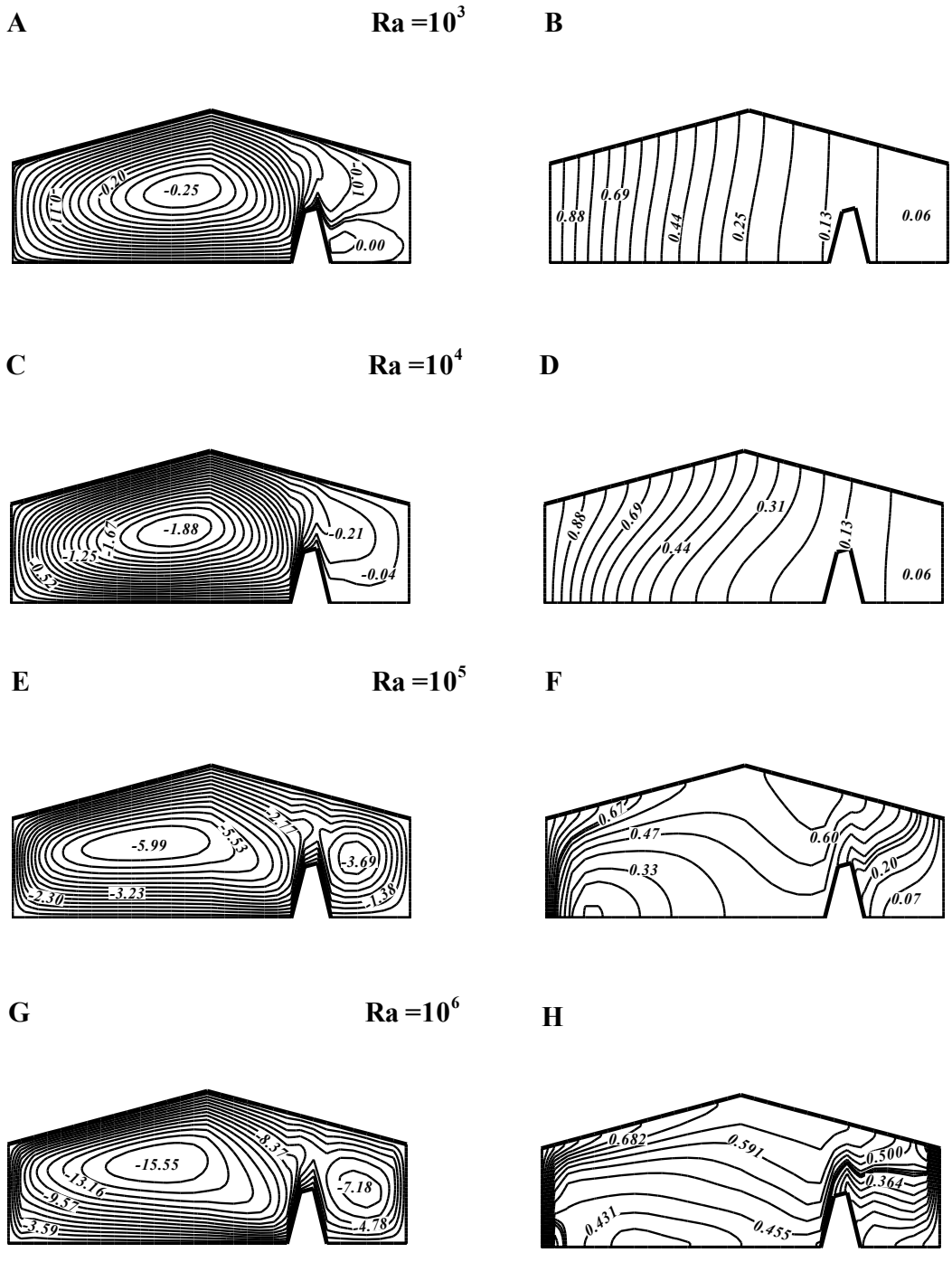

Fig. 5 Rayleigh number effect on streamlines (left side) and isothermal contours (right side) in the typical cavity for case 1, baffle attached the horizontal bottom wall at LB=0.75L, HB=0.4H*

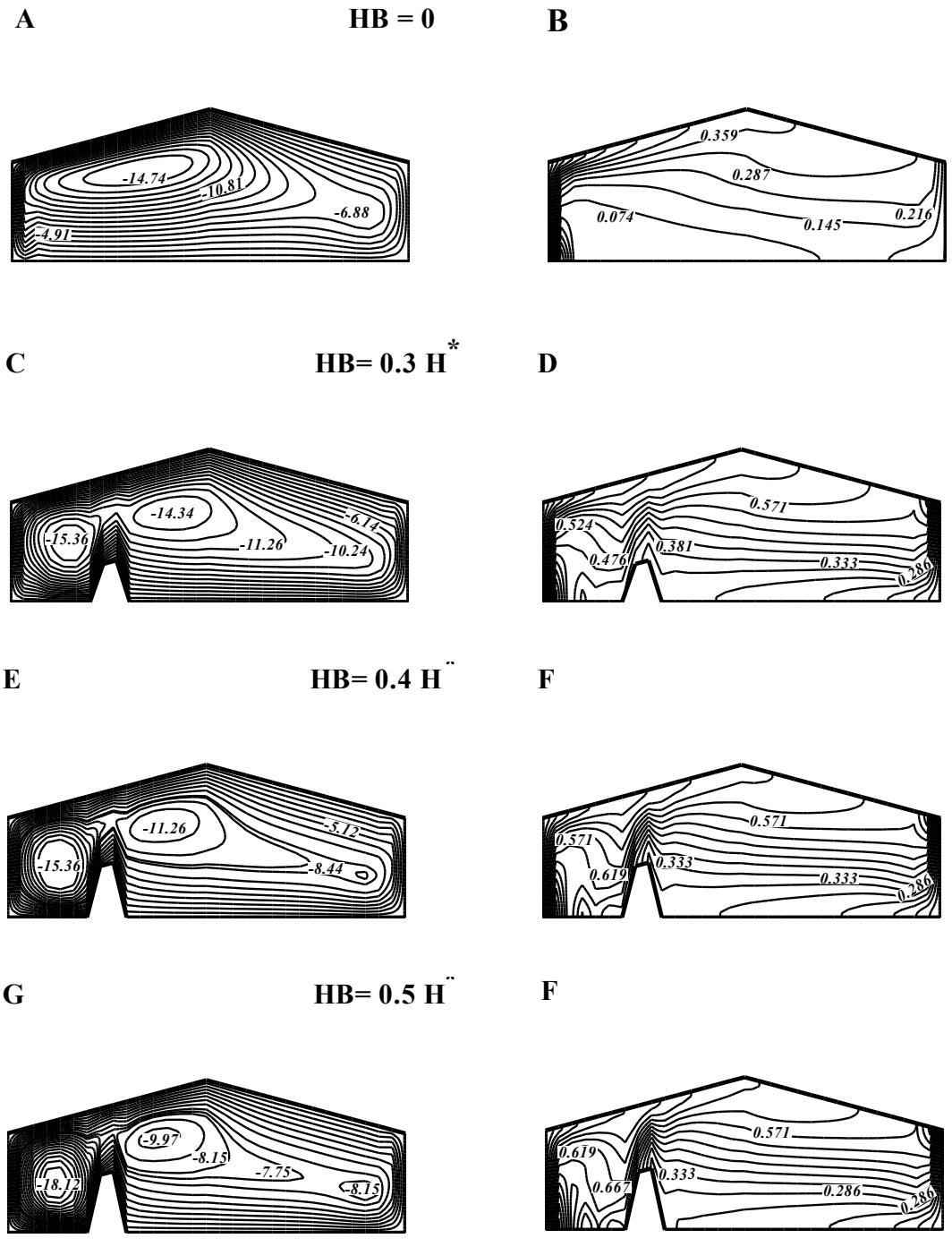

Fig. 6 Baffle height effect on streamlines (left side) and isothermal contours (right side) in the typical cavity for case 1, baffle attached the horizontal bottom wall at LB=0.25L, Ra=10^6

Fig. 7 Rayleigh number effect on streamlines (left side) and isothermal contours (right side) in the typical cavity for case 2, baffle attached the upper inclined wall at LB=0.25L, HB=0.4H*

A **Ra =10^3** **B**

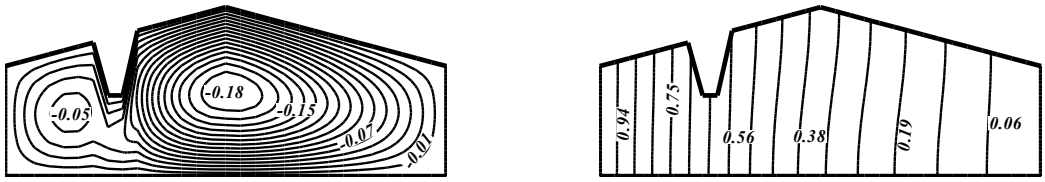

C **Ra =10^4** **D**

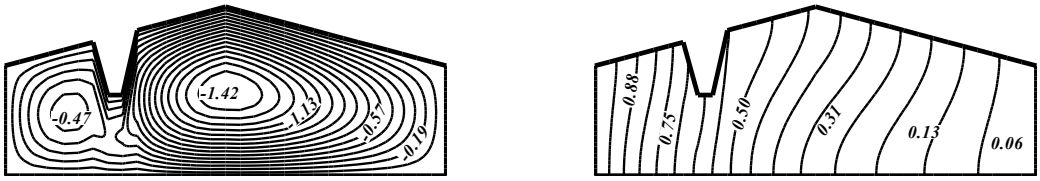

E **Ra =10^5** **F**

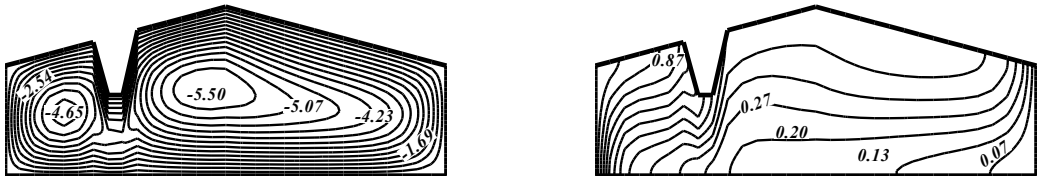

G **Ra =10^6** **H**

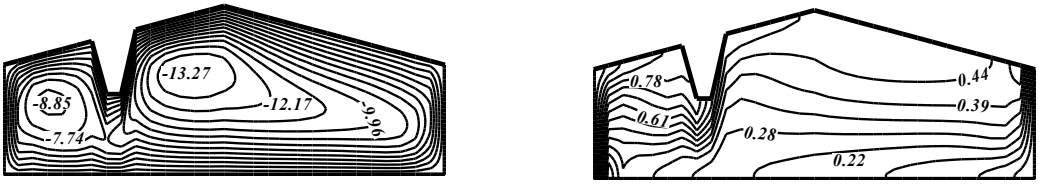

Fig. 8 Rayleigh nu
contours (right sid
uppe

A **Ra =10^3** **B**

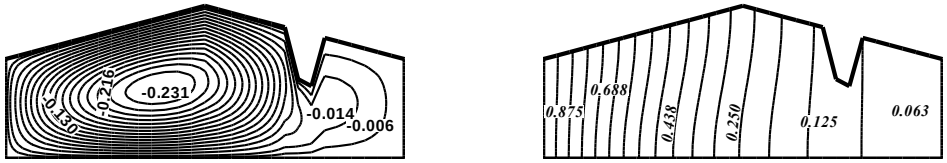

C **Ra =10^4** **D**

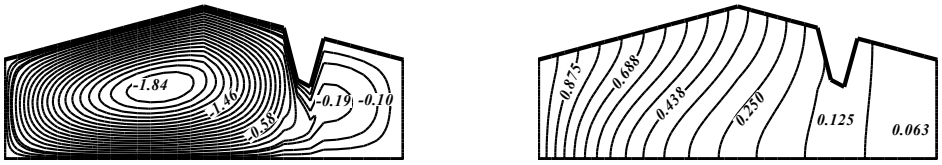

E **Ra =10^5** **F**

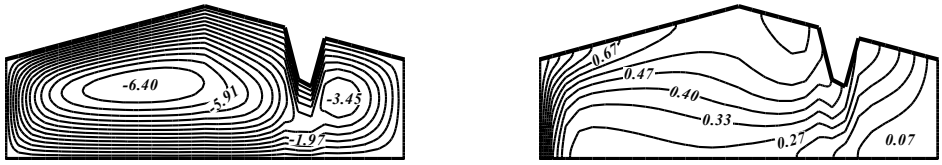

G **Ra =10^6** **H**

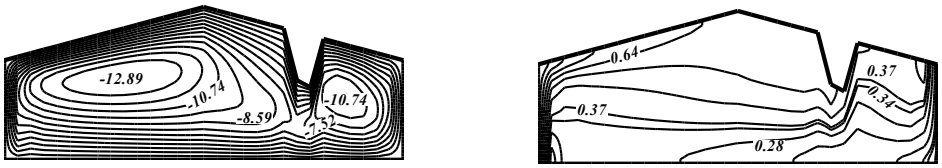

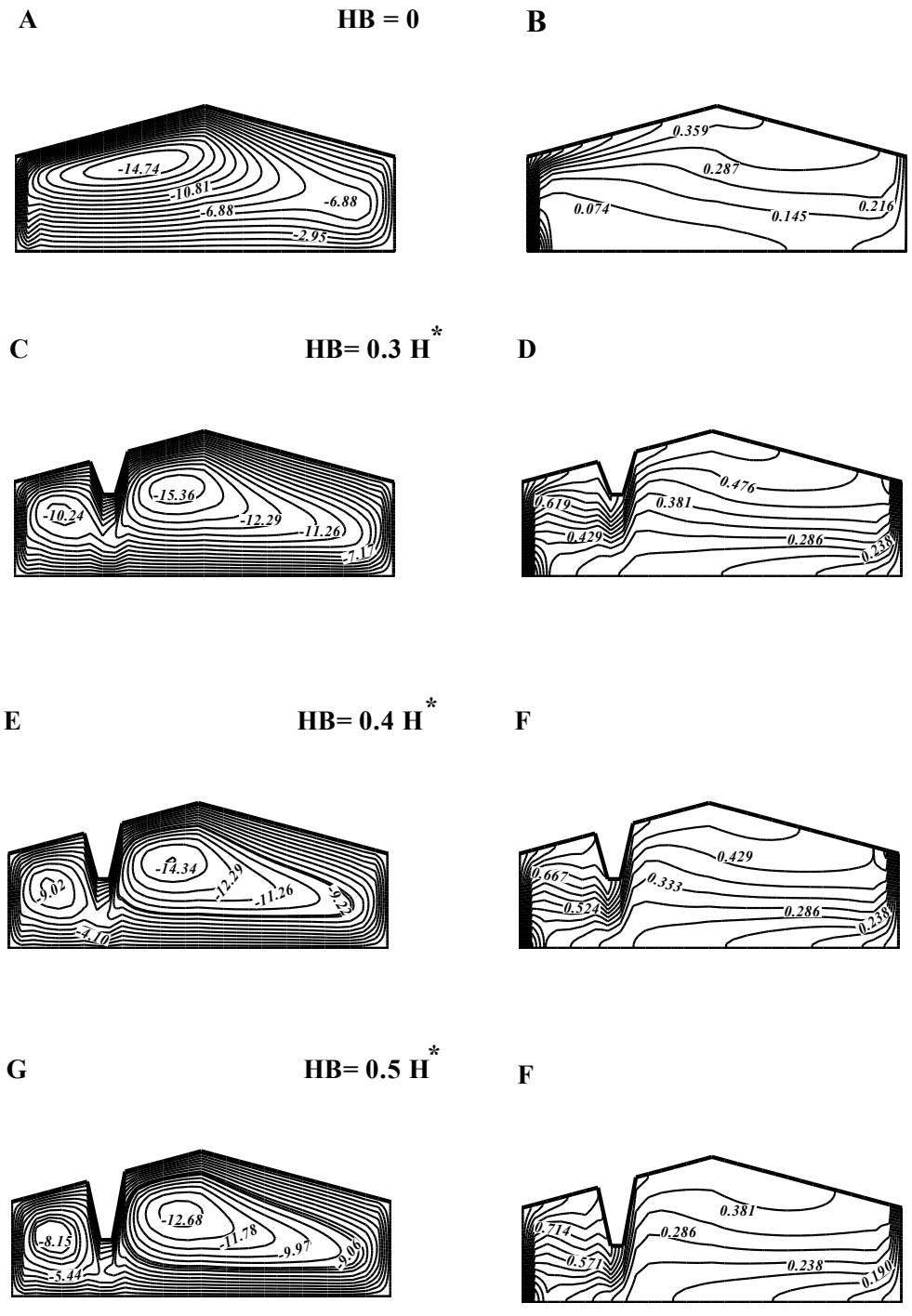

Fig. 9 Baffle height effect on streamlines (left side) and isothermal contours (right side) in the typical cavity for case 2, baffle attached the upper inclined wall at LB=0.25L, Ra=10^6

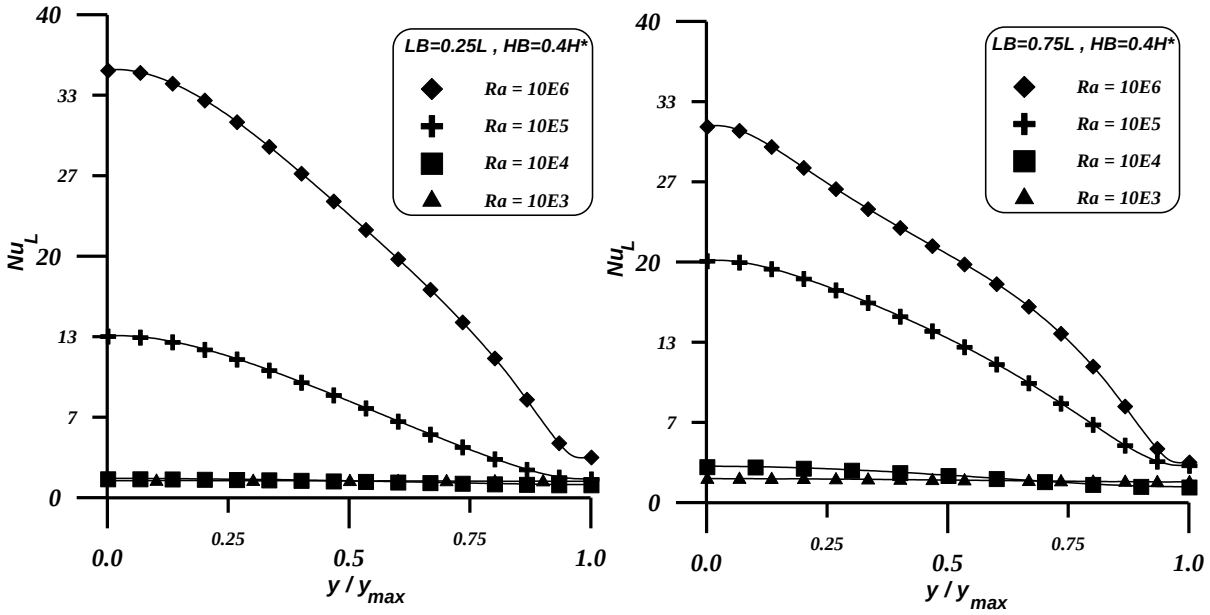

Fig. 10 Local Nusselt number distribution on the left hot wall for case 1, baffle attached the horizontal bottom wall of the cavity

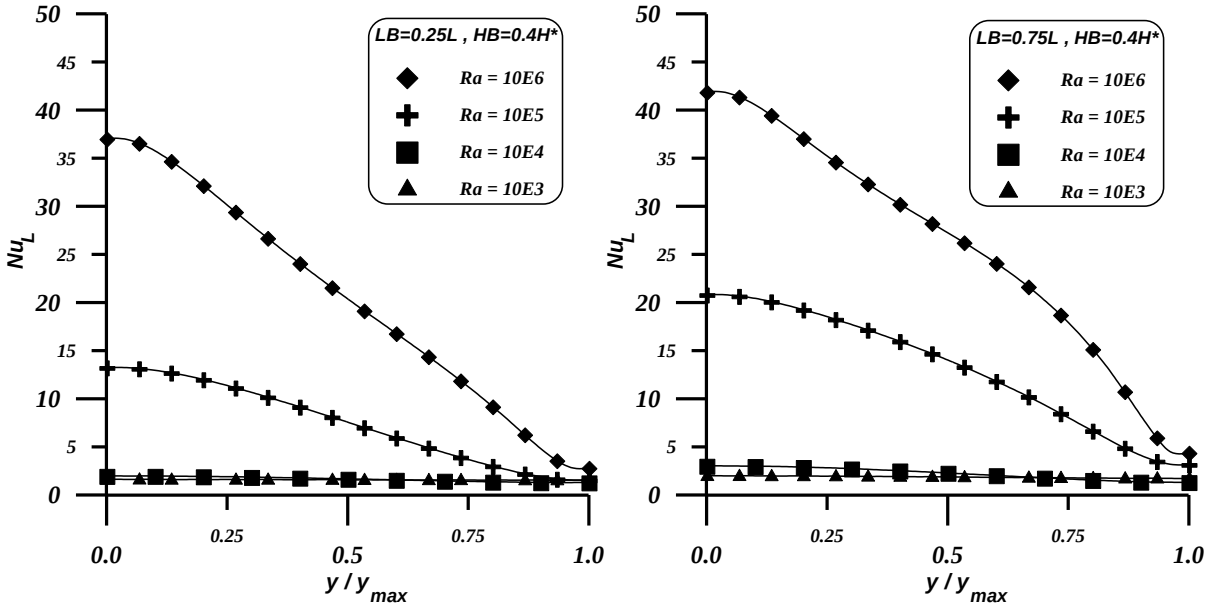

Fig. 11 Local Nusselt number distribution on the left hot wall for case 2, baffle attached the upper inclined wall of the cavity

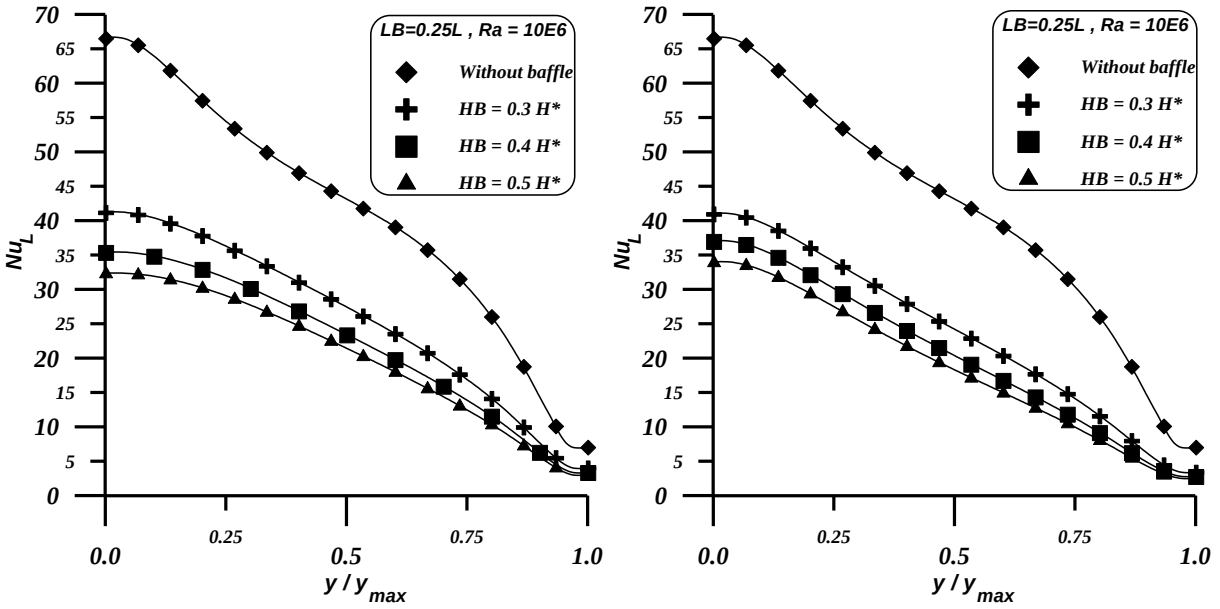

Fig. 12 Local Nusselt number distribution on the left hot wall for Ra = 10^6.
A. Case 1, baffle attached the horizontal bottom wall.
B. Case 2, baffle attached the upper inclined wall.

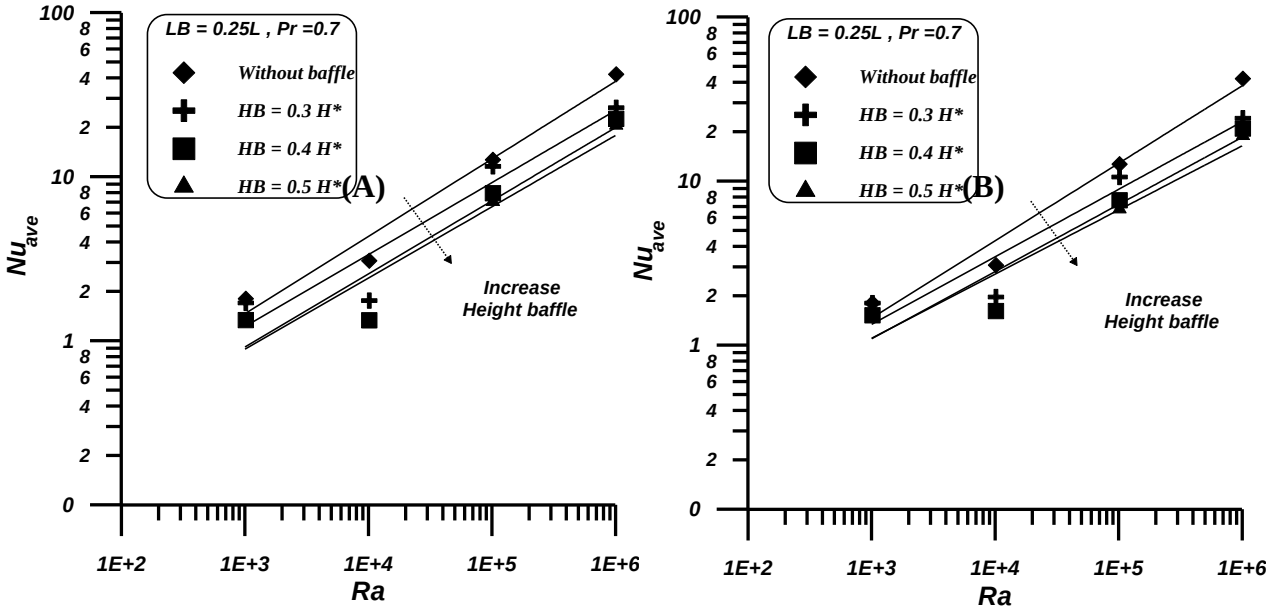

Fig. 13 Average Nusselt number distribution with Rayleigh number on the left hot wall
A. Case 1, baffle attached the horizontal bottom wall.
B. Case 2, baffle attached the upper inclined wall.